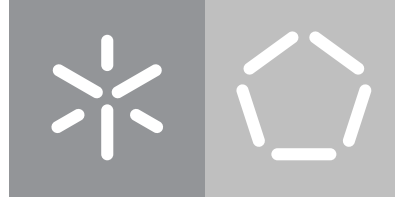


Universidade do Minho
Escola de Engenharia

André Agostinho Ribeiro Campos

ALFA-Pd::
Hardware-assisted LiDAR Point-Cloud Denoising.



Universidade do Minho
Escola de Engenharia

André Agostinho Ribeiro Campos

ALFA-Pd::
Hardware-assisted LiDAR Point-Cloud Denoising.

Dissertação de Mestrado
Engenharia Eletrónica Industrial e Computadores
Sistemas Embebidos e Computadores

Trabalho efetuado sob a orientação do(a)
Professor Joao Monteiro
Professor Tiago Gomes

dedicatory

Acknowledgements

Abstract

Resumo

Contents

List of Figures	vii
Acronyms	viii
1 Introduction	1
1.1 Motivation	1
1.2 Main Goal	1
1.2.1 Objectives	1
1.3 Dissertation Structure	1
2 State of the Art	2
2.1 LiDAR	2
2.1.1 LiDAR Working principle	3
2.1.2 LiDAR Optical Architectures	4
2.2 LiDAR in the automotive world	7
2.2.1 On-Road measurements	8
2.2.2 Driving Assist	8
2.2.3 Pedestrians Recognition	8
2.2.4 Weather influence	9
2.2.5 LiDAR vulnerabilities	11
2.3 LiDAR development platforms, and simulators	12
2.3.1 Analog Devices AD-FMCLIDAR1-EBZ	12
2.4 Denoising Filters	14
2.4.1 Conventional noise filter.	14
2.4.2 State fo the art filters:	15
2.4.3 Filters Study	16
2.4.4 Results	20
3 Platform and tools	21
3.1 ALFA	21
3.2 ROS	21

3.3	Zynq UltraScale+ MPSoC ZCU104	21
3.4	PCL	21
4	ALFA-Pd Architecture	22
4.1	ALFA-DVC	22
5	ALFA-Pd Framework	23
6	Evaluation and Result	24
6.1	Filter performance	24
6.2	Hardware versus Software	24
7	Conclusion	25
7.1	Future work	25
	Bibliography	26

List of Figures

2.1	LiDAR Working principle.	3
2.2	CW-iToF scheme.	4
2.3	PM-iToF scheme.	4
2.4	Velodyne VLP-16(left), Velodyne HDL32(Right).	5
2.5	Velodyne Vellaray H800.	5
2.6	Flash LiDAR.	6
2.7	1D Scanning LiDAR.	6
2.8	2D Scanning LiDAR.	6
2.9	Automotive LiDAR evolution.	8
2.10	AD-FMCLIDAR1-EBZ prototyping platform.	12
2.11	AD-FMCLIDAR1-EBZ: DAQ board.	13
2.12	AD-FMCLIDAR1-EBZ: Laser board.	13
2.13	AD-FMCLIDAR1-EBZ: AFE board.	13
2.14	Software tool.	16
2.15	Voxel filter results.	17
2.16	ROR filter results.	17
2.17	SOR filter results.	18
2.18	FCSOR filter results.	19
2.19	DROR filter results.	19

Acronyms

ABS	Anti-lock braking system.
ADAS	Advanced driver-assistance systems.
APD	Avalanche Photodiode
CW-iToF	Continuous-Wave modulation Indirect Time of Flight.
DoS	Denial-of-service.
dToF	Direct Time of Flight.
ESC	Electronic stability control.
FoL	Field of Light
FoV	Field of View.
GNSS	Global navigation satellite system.
iToF	Indirect Time of Flight
LiDAR	Light Detection And Ranging.
ODOA	Obstacle detection and avoidance.
PM-iToF	Pulse Modulation Indirect Time of Flight
SNR	Signal-to-Noise Ratio
TCS	Traction control system.
TIA	Trans-impedance Amplifiers
ToF	Time of Flight.

Introduction

1.1 Motivation

1.2 Main Goal

1.2.1 Objectives

1.3 Dissertation Structure

State of the Art

2.1 LiDAR

LiDAR stands for "Light Detection And Ranging" and is a method for measuring distances by illuminating the target with laser light and measuring the reflection with a sensor. LiDAR is commonly used to make high-resolution maps with diverse applications like surveying, geodesy, geomatics, archaeology, geography, geology, geomorphology, seismology, forestry, atmospheric physics.

Obtaining distances through measuring travel-time and intensity of light beams date back to the pre-laser decade in 1930 ([Synge, 1930], [Tuve et al., 1935]) but only in 1953 that the concept of Light detection and ranging(LiDAR) appeared, which was initially a portmanteau of light and RADAR [Ring, 1963] and introduced in [Biswas and Middleton, 1971].The LiDAR principle carried out through time unchanged, it can measure distances by using round-trip time of a flight pulse traveled between the sensor and a target. Between the first appearance of a LiDAR system and now the evolution was focused on the improvement of components, without the appearance of new disrupting techniques.

LiDAR can also provide more information than the three dimensions(x,y,z), it can provide the physical time(t) dimension from repeat LiDAR acquisition and laser return intensity data dimension based on the brightness of single- or multi-wavelength laser returns. An application based on this information is studied in [Eitel et al., 2016], where the author touch topics related to the subjects: earth and ecological sciences(EES) with a special focus in geology, glaciology, hydrology, biogeochemistry, and terrestrial ecology. Another interesting article is [Burt et al., 2018], where the author studies plants ecology where LiDAR is used to the retrieval of traditional parameters of forest structure such as stem diameter, tree height, empirical testing of plant form, function hypotheses. The author developed a software to automatic extraction of tree-level point clouds from larger-area point clouds. However in order for this software to run its needed a supercomputer with 24-core 2.40 GHz Intel Xeon E5-2620v3 (15 MB L3 cache) node with 72 GB DDR4 RAM and mechanical hard drive .Despite this 2 days and a week are needed to finish.

In terms of embedded systems, there are articles like [Rakotovao et al., 2016] where the author present a solution for microcontrollers without floating-point unit or even FPGA, this work is for the use of LiDAR systems in some robot applications.

2.1.1 LiDAR Working principle

The working principle of LiDAR systems stayed untouched through time and it consists on measuring distances by calculating the round-trip travel time of a light signal emitted by a laser and reflected by the target object, also known by time of flight(ToF). To read the ToF, LiDAR systems are composed of an emitter, that transmits the laser signal, and a receiver that receives the back-scattered signal.

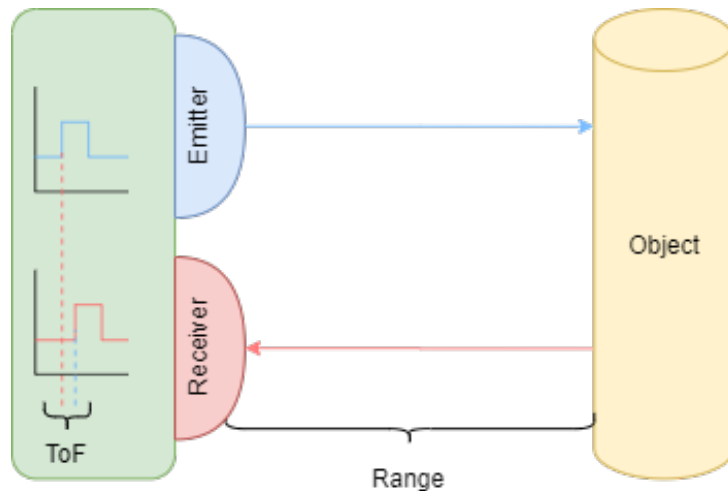


Figure 2.1: LiDAR Working principle.

In order to calculate the range, LiDAR systems use the following mathematical equation:

$$R = \frac{1}{2}c\tau \quad (2.1)$$

In the equation, c is the speed of light in the medium, and τ is the time of flight between the sensor and the target. This is the calculation for a single point, but nowadays LiDAR systems are capable of 3D representations. This is achieved by a predetermined field of view (FoV) and the ToF is calculated for each point. To calculate ToF there are two methods, one is the Direct Time of Flight(dToF) and is described in 2.1, the other is Indirect Time of Flight(iToF).

dToF calculates ToF based on the signal's pulses and detected reflection. This comes with several advantages like implementation simplicity, as it does not take signal's phase into consideration, and it is much cheaper and smaller when compared to other solutions. However, due to the simplicity of the emitter and receiver, measuring ToF comes with low accuracy, and because of external light sources, the measurement results in a lower signal-to-noise ratio (SNR).

iToF is a more complex technique, but despite that is surely the most mature silicon-based ToF technology with many commercial implementations on the field. Indirect Time of Flight is divided into two technics, continuous-wave modulation (CW-iToF) and pulse modulation (PM-iToF).

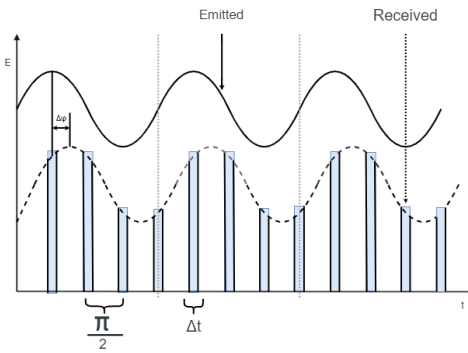


Figure 2.2: CW-iToF scheme.

CW-iToF [Süss et al., 2016] is typically measured by multiple short-time integrators of duration δt which are mutually displaced by $\pi/2$ in order to yield four orthogonal samples. These four samples hold the data of depth, reflectivity, and ambient level, which can all be resolved as they are independent.

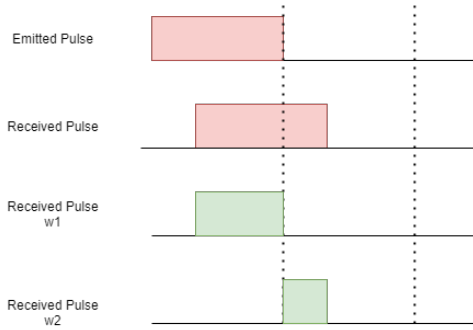


Figure 2.3: PM-iToF scheme.

PM-iToF [Süss et al., 2016] technique is based on the signal reflected ratio in a series of integrating windows where the signal is modulated in form of a pulse. Because of the integrated window, the reflected pulse often comes in different integrated windows as shown in figure 2.3 enabling the possibility to calculate the ToF. This technique is often implemented with a CCD/CMOS sensor as they provide charge accumulation and storage capability enabling high-resolution depth imaging and fixed optics. PM-iToF technique comes with other advantages such as reduced laser requirements, as it integrates optical energy, disregarding wavelength.

iToF technique, alike everything, comes with a cost associated. The range is significantly lower because longer ranges require longer pulses that are bad for SNR or range gates that influence frame rate. There is also a Multi-object Disambiguation problem because the computed distance is an average of all sources of optical reflection. SNR can also be low because CCD/CMOS detectors don't typically provide gain, can have a low fill factor, and has lower responsivity than the standard photodiodes used in dToF.

2.1.2 LiDAR Optical Architectures

In order to recreate surrounding images using LiDAR systems several techniques were developed, being categorized into two main groups, the ones that use some kind of beam-steering to scatter a light

signal across the environment, and the ones that don't use any mechanical part at all, emitting a light signal for all environment simultaneously.



Figure 2.4: Velodyne VLP-16(left), Velodyne HDL32(Right).

LiDAR systems with beam-steering mechanisms are often categorized as rotor-based mechanical LiDARs [Atanacio-Jiménez et al., 2011]. This is the most mature technique being found on a lot of LiDAR systems on the market. To achieve 360° horizontal detection, it employs a mechanical rotor to spin the scanning part of the system. Vertically, the field of view is only limited by the number of emitter/receiver pairs, but scaling these pairs increases the cost significantly. Because it has mechanical parts, the frame rate is affected, slowing down the performance of these systems.



Figure 2.5: Velodyne Vellarray H800.

Scanning Solid-State LiDAR systems [Raj et al., 2020] are the complete opposite of the rotor-based mechanical ones. These systems don't have any mechanical parts, therefore they have a limited FoV, but on the other hand, they are cheaper because of the lower complexity that these systems have. The lower complexity also means that they are faster than the others, having a higher frame rate. Due to their scalability in the automobile world, they are often used in a group of sensors in order to increase FoV and be able to match the mechanical ones.

Flash LiDAR

Flash LiDAR systems can be considered solid-state because they don't have any moving parts. These systems typically use a flash to illuminate the environment, similar to standard digital cameras, and to receive the signals, it has photodetectors that collect the reflected light (2.6). Because of the way the light is emitted, one can say that the field of light (FoL) is roughly equivalent to the Field of View(FoV), being only limited by the receiver that establishes the resolution of the FoV. These systems are considered the cheapest ones compared to the others, having the fastest frame rate due to the lack of moving parts. Frame rates are not the only advantage obtained by this system, being immune to light distortion because

all FoV points share the same light source. To increase range in Flash LiDARS one needs to increase laser power, and due to power limitations, Flash LiDARS have a smaller range in comparison to the other LiDAR types.

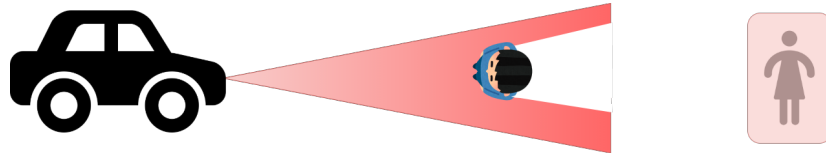


Figure 2.6: Flash LiDAR.

2D Scanning LiDAR

2D Scanning LiDAR systems start to focus light in a beam to illuminate differing of flash LiDAR (2.7). The emitter of these systems has a low divergent laser with some beam steering mechanism, this emitter sets the resolution in one dimension. The receiver no longer is responsible for all the FoV resolution, instead, it is responsible for setting the resolution in the other dimension. These techniques enable longer-range depending only on the optics of the system, it is also a very flexible architecture, but because the FoV point doesn't share the same light source anymore, these systems begin to suffer some interference lowering the SNR.

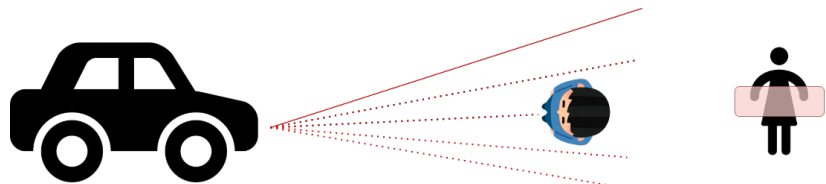


Figure 2.7: 1D Scanning LiDAR.

3D Scanning LiDAR

3D Scanning LiDAR systems are very similar to 1D Scanning LiDAR systems, but with complex beam steering systems enabling it to scan in both dimensions, x and y (2.8). These systems are the ones capable of achieving the longest range, but, they are the most expensive ones because these systems have incredible complex beam steering systems, these beam steering systems also compromise the frame rate, having a very low frame rate compared to flash LiDAR's

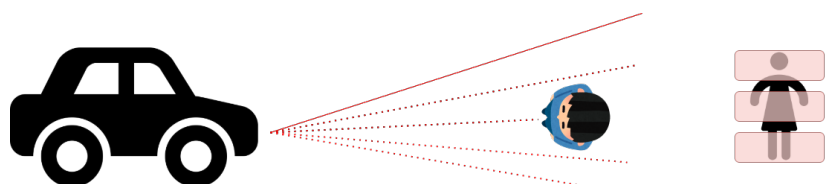


Figure 2.8: 2D Scanning LiDAR.

2.2 LiDAR in the automotive world

LiDAR is an active sensors that illuminate the surroundings by emitting lasers. Ranges are measured precisely by processing the received laser returns from the reflecting surfaces. One of LiDAR's competitors is camera-based approaches that despite much progress in processing methods still estimate distances. This approach encounters difficulties when estimating distances for cross-traffic entities, particularly for monocular solutions ([Li and Ibanez-Guzman, 2020]).

Currently, many high-level autonomous vehicles use LiDAR systems as part of their perception systems despite their high cost and moving parts. The output of a perception system comprises the following three levels of information: "Physical description" which consists of the pose, velocity, and shape of objects, "semantic description" that categorizes objects and "intention prediction" that predicts the likelihood of an object's behavior. With this in mind, LiDAR systems outputs are commonly used for object detection, classification, tracking, and intention prediction, but there is a catch, the semantic information carried by LiDAR is more or less difficult than the one that is acquired from a camera, a contextual sensor is good at object recognition. In practice, LiDARs are combined with cameras to complement each other. A camera is weak in distance estimation, while LiDAR is inadequate for object recognition. Precise physical and semantic information, together with map information, will improve intention prediction without any doubts([Li and Ibanez-Guzman, 2020]).

The commonly used LiDAR operate by scanning its field of view (FoV) with one or several laser beams. The laser beam is generated by an amplitude-modulated laser diode that emits at near-infrared (NIR) wavelength. The laser beam is reflected by the environment back to the scanner. The signal received is filtered and the difference between the transmitted and received signals is measured, which is proportional to the distance. The difference in variation of reflected energy due to surface materials is compensated through signal processing([Li and Ibanez-Guzman, 2020]).

A LiDAR system can be partitioned into the laser rangefinder system and the scanning system. The laser rangefinder comprises the laser transmitter which illuminates the target via a modulated wave, and then there is the scanning system that includes the photodetector, which generates the electronic signal from the reflected photon after optical processing and photoelectric conversion. The optics collimate the emitted laser and focus the reflected signal onto the photodetector, and for last, there are signal processing electronics that estimates the distance between the laser source and the reflecting surface ([Li and Ibanez-Guzman, 2020]).

In the figure, 2.9, one can see a timeline of development stages, this was done by analyzing the most cited articles through the years until the day of writing. The first work that appeared in the automotive world related to LiDAR was about measuring emissions on the road. Time went flying and one can see that LiDAR was started to be integrated into driving assistance systems with the goal to lower road accidents. The next step was ADAS where cars have the capability of driving autonomously on the highway. With the fast evolution of LiDAR systems, safety was a must, and so, studies about pedestrian recognition started to appear to better identify and avoid people on the road. LiDAR systems need to operate in extreme weather

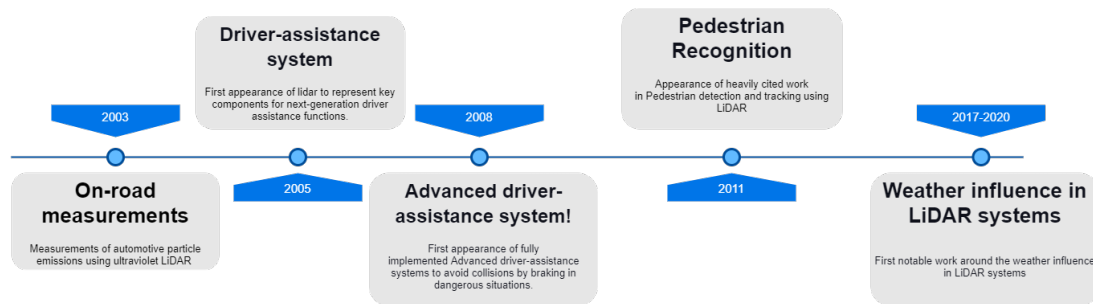


Figure 2.9: Automotive LiDAR evolution.

conditions, and because of that, most current studies are about the influence of weather in those systems.

2.2.1 On-Road measurements

There is a lot of research being done all around the world about LiDARs in the automotive world, one of the oldest article about this subject is [Raschofer and Gresser, 2005] where the author says that automotive radar and LiDAR sensors represent key components for next-generation driver assistance functions. This is an article ahead of its time because some premiums cars are starting to get features like cruise control and this article talks about fully autonomous cars. It also approaches why cars should have radars and LiDARs to implement new features like driving assistance. In 2003 LiDAR was used to do on-road measurements of automotive particle emissions using ultraviolet LiDAR [Moosmüller et al., 2003].

2.2.2 Driving Assist

In 2008 an anticolision system called "PROFETA" using LiDAR to do the object detection was developed [Isermann et al., 2008] where the main goal is to avoid collisions by braking the vehicle automatically in dangerous situations. In year after, there are two more articles published about anti-jamming [Gong et al., 2009] [Lindner and Wanielik, 2009]. With this information, one can see that around 2008/2009 was the time where the idea of autonomous driving was emerging in the automotive industry, starting to do some basic recognition of the environment in the attempt to predict and avoid possible collisions. There is work around adaptive cruise control at this time too [Pananurak et al., 2009]. Adaptive cruise control is a cruise control advanced driver-assistance system for road vehicles that automatically adjusts the vehicle speed to maintain a safe distance from vehicles ahead.

2.2.3 Pedestrians Recognition

Since 2011 we start to see some work about pedestrian detection and tracking using LiDAR systems. In [Ogawa et al., 2011] the author compares LiDAR to a camera to see which one was the best at pedestrian recognition with the goal to help reduce traffic accidents involving pedestrians.

Until 2017 there aren't many relevant articles about pedestrian tracking, but in 2017 some articles start to emerge again. In [Granstrom et al., 2017] the author tries to improve previous work [Lundquist et al., 2013]

in order to achieve the best performance especially in challenging scenarios using a sampling-based method for data association approximation in multiple extended target tracking, called stochastic optimization.

In [Patole et al., 2017] the author made a review article where it summarizes various aspects of automotive radar signal processing techniques, including waveform design, possible radar architectures, estimation algorithms, implementation complexity-resolution trade-off, and adaptive processing for complex environments, as well as unique problems associated with automotive radars such as pedestrian detection. Even though this article main focus is radar technology a lot of the concepts discussed in this article can be applied to LiDARs as well, for example, to identify pedestrian walking we can check the small change in range, this small changes produces very low Doppler shift. In other words, the micromotion of a target produces what is known as a micro-Doppler. Likewise, the periodic motion of limbs creates a periodic pattern in velocity over time, which is also known as the micro-Doppler signature. This signature is greatly investigated in [Guo Liren et al., 2015].

Pedestrian recognition is a very important subject, and it can be seen in this article [Zhou and Sun, 2019], where the author writes about safety, inspired by the first death that a self-driving vehicle, Elaine Herzberg on March 18, 2018, that was hit by a self-driving Uber SUV.

2.2.4 Weather influence

One downside of LiDAR technology is that it can be influenced a lot by external factors like weather, in fact, there is another article from one author already cited previously about this issue [Raschofer et al., 2011] where there is a good overview of the different physical principles responsible for laser radar signal disturbance and theoretical investigations for estimation of their influence. This is an enormous problem for LiDARs, and because of this there is also a lot of work around this. In [Hasirlioglu et al., 2016] the author starts by referencing some facts about traffic accidents, like each year over 1.2 million people die in traffic accidents, to show why we need some kind of drive assistance to prevent human deaths, and then explores how the environment influences the accuracy of the sensors systems. Still in the year 2016, we have another article about the influence of harsh weather conditions having future autonomous cars in mind [Kutila et al., 2016]. In this article, the author claims that the LiDAR sensor tested degrades his performance by 25% in harsh conditions like fog.

First, one needs to understand what fog is, and this author describes fog as a complex phenomenon characterized by multiple factors such as droplet microphysics, aerosol chemistry, radiation, turbulence, large/small-scale dynamics, and droplet surface conditions. In other words, fog is a collection of small water droplets in the air, with diameters less than 100 μm . Important note by the author is that foggy conditions differ when comparing fog at sea, in the atmosphere, and on the ground. The droplet size on the ground is smaller compared to fog droplets in cumulus clouds. One of the conclusions in this article is that stabilizing all possible conditions is too cumbersome for any practical outdoor application where ambient illumination, fog density, snow, etc. are a reality. Furthermore, the author says there are two major development steps planned to increase the robustness, of the LiDAR system in automotive use in order to

increase the level of autonomous driving in all weather conditions: "Improve the laser scanner hardware by investigating the optimal wavelengths, possible power ranges and optimizing optical and electronic components." and "Develop a software module, which continuously assesses the performance level of the laser scanner according to the obvious changes in detection capability."

In 2017, the article [Hasirlioglu et al., 2017] there is work concerning fog simulation to test performance, as it is known that fog has a negative influence on wave propagation, especially in the visible range. Hence, surround sensors must be tested under realistic conditions. First, one needs to know the influences of fog on optical communication and for that one has Kruse model ([Redington, 1962]) that predicts the specific attenuation using the local visibility and is given by:

$$\text{Attenuation} = \frac{3.91}{V} \left(\frac{\lambda}{\lambda_0} \right)^{-q}, (\text{dB/km})$$

Where V is the visibility in km, λ the wavelength in nm, λ_0 the visibility reference wavelength (550 nm), and q the coefficient related to particle size distribution in the atmosphere, q depends on visibility and can be calculated as follows:

$$q = 0.585V^{\frac{1}{3}} \text{ for } V < 6 \text{ km.}$$

The results provided by the author show that it is clear that with an increasing number of activated fog layers, the disturbance increases. The influence of small water particles in the air is most visible on a dark background. The fog influence is less visible on bright background.

One can conclude that the influence of weather in LiDAR performance is an important subject when there is work through the years until the present date. The analysis of weather influences on the performance of LiDAR sensors and weather detection are important steps towards improving safety levels for autonomous driving in adverse weather conditions by providing reliable information to adapt vehicle behavior. In 2019 there is work in [Heinzler et al., 2019] where the author present an in-depth analysis of automotive LiDAR performance under harsh weather conditions like heavy rain and dense fog. For LiDAR sensors, the most challenging environmental conditions are bright sun, fog, rain, dirt, and spray. The author concludes that the detection quality and range is expected to be impaired as significant laser power is scattered by the atmospheric particles, leading to the other echoes. The environment perception and the range of the sensor are limited. Only a few secondary echoes can be associated with the fog as most coincide with the position of the car. In dense fog (visibility at 20-40m) the environment perception is highly limited. Nearly all primary echoes are observed at a range of fewer than 5 m and thus caused by the fog. Nevertheless highly reflecting targets like the retroreflectors of the taillights are still correlated with secondary or tertiary echoes. Echoes exist because a drawback regarding Automotive LiDAR systems is that they usually use monochromatic unpolarized light and measure only elastic scattering effects. This is compensated in some systems by providing multi-target detection (multiple echoes), which facilitates the differentiation of detections caused by rain, fog, or snow from those caused by solid objects.

In [Goodin et al., 2019] the author does a quantitative study on how rain-rate influences ADAS performance by developing a mathematical model for the performance degradation of LiDAR as a function of rain-rate and incorporate this model into a simulation of an obstacle-detection system to show how it can be used to quantitatively predict the influence of rain on ADAS that use LiDAR. In this article, the author concludes that the resulting point cloud is drastically affected by the increasing rain rate. However the LiDAR range reduction does not have as strong of an impact on the detection range for the obstacle, meaning that the capability of the sensor to detect the obstacle is clearly dependent on factors other than the rain.

Weather influence in LiDAR systems has ongoing research and there is recent work to prove this, in [Byeon and Yoon, 2020] the author addresses the impact of rain on the LiDAR system by considering the raindrop distributions of different regions as, when light encounters raindrops in the air, various physical phenomena occur. These phenomena can be understood by considering the raindrops as particles. In general, particles illuminated by light demonstrate reflection and refraction, absorption, and scattering.

In [Vargas Rivero et al., 2020] the author's goal is to identify local weather information to recognize if it is working inside its operational design domain and adapt itself accordingly. The author tries to identify weather with LiDAR systems but acknowledges that there are different alternatives to evaluate current weather and road friction in the vicinity of a car by the use of information provided by the vehicle's windshield wipers, fog lights, torque, speed of engine and tires, anti-lock braking system (ABS), electronic stability control (ESC) and traction control system (TCS) intervention events, temperature, global navigation satellite system (GNSS) position, steering wheel angle and braking signal. The author concludes that it is possible to use an automotive LiDAR sensor to differentiate between four different weather types: Clear, Rain, Fog, and Snow.

2.2.5 LiDAR vulnerabilities

In [Shin et al., 2017] the author exposes different vulnerabilities that a LiDAR can have. In this article, the author was able to inducing fake dots closer than the spoofer(attacker) location and create a saturation attack against LiDARs which can incapacitate a LiDAR from detecting objects. The principle of saturating or denial-of-service (DoS) is to push the overall level of the input signal into the saturation region, in order to render the sensor unable to reflect the variations in the legitimate input signal. An attacker can incapacitate a sensor by exposing it to excessive stimuli.

In the spoofing attack, the goal of the sensor spoofing is to deceive the victim's sensor by exposing it to the attacking signal which simulates the circumstance that the attacker wants the sensor to believe. Simulating a fake circumstance exploits the semantic gap between what the circumstance really is and how the sensor perceives it to be. An active sensor can take a particular waveform (ping waveform) to differentiate its echoes from the other inbound signals. Therefore, the attacker should first acquire the ping waveform, and then relay it after an intentionally inserted delay to affect the victim sensor; this is called sensor spoofing by relaying. Besides, the received ping waveform can be duplicated during relaying, to

amplify the effect.

2.3 LiDAR development platforms, and simulators

LiDAR systems are having an increase popularity in the automobile world, resulting in an increased demand for those systems. As a result development boards and simulators started to appear in the market in order to speed up LiDAR systems development by providing platforms where algorithms can be tested and debugged.

2.3.1 Analog Devices AD-FMCLIDAR1-EBZ

In 2019, Analog devices released their first prototyping platform. The AD-FMCLIDAR1-EBZ(2.10) [?] is a modular hardware platform for 1D non-Scanning LiDAR development. Due to its modular approach, it allows the flexibility to meet individual design needs, reducing time to market and complexities of LiDAR development. It can be paired with an FPGA through a FMC HPC connector.



Figure 2.10: AD-FMCLIDAR1-EBZ prototyping platform.

The AD-FMCLIDAR1-EBZ prototyping platform is divided into three modules: Data Acquisition(DAQ) Board, Laser Transmitter Board, and the AFE Receiver board.



Figure 2.11: AD-FMCLIDAR1-EBZ: DAQ board.

The DAQ board(2.11) is a high-speed data acquisition board containing a quad-channel ADC and clocking control for the full system. This board is the one responsible for the connections between the FPGA and the kit through a FMC HPC connector. This board is where the analog-to-digital conversion is completed and sent via JESD Interface. Additionally, all the digital signals between the FPGA carrier board and AFE and laser board pass through the DAQ board, going to two 100 pins high-speed connector that is similar in both boards (AFE and laser board) using a ribbon cable. The ADC channels use a SMA cable to connect with the corresponding signal sources on the AFE and Laser boards.



Figure 2.12: AD-FMCLIDAR1-EBZ: Laser board.

The laser board(2.12) contains 4 individual lasers with the appropriate precision driver and power components for accurate firing of the laser. This board generates the optical pulses with a wavelength of 905nm, driving all lasers simultaneously for an increase in beam strength providing a longer range. It uses a PWM signal generated by the FPGA carrier board with programmable pulse width and frequency.



Figure 2.13: AD-FMCLIDAR1-EBZ: AFE board.

The AFE board(2.13) contains a 16 channel APD and four quad-channel trans-impedance amplifiers with the necessary power and timing signal chains. Also, custom optics can be fitted using a standard

mounting adapter depending on the individual use case. This board is the one responsible for receiving the optical reflected signal and convert it to an electrical signal and transferring them to an ADC on the DAQ board. This optical signal is converted using a 16 channel APD, and the output is fed to four low-noise four-channel trans-impedance amplifiers with 220MHz bandwidth.

2.4 Denoising Filters

In order to accelerate denoising algorithms, a study of the conventional and current state of art filters needs to be made.

2.4.1 Conventional noise filter.

There are 3 mature filter methods to remove noise from point clouds, radius outlier removal (ROR), statistical outlier removal (SOR), and voxel grid (VG) filters [Rusu and Cousins, 2011],[Han et al., 2017]. The outlier removal consists of classifying every point as an inlier or an outlier, and remove the outlier, and to do this different algorithms were implemented. However, the outlier removal algorithms when applied to 3D LiDAR point clouds show some limitations in terms of speed and accuracy.

2.4.1.1 ROR

The working principle of the ROR filter is very simple, for every point, it computes the mean distance to its neighbors within a user-defined radius by using a k-d tree data structure. If the number of neighbors within a specified radius is below the user-defined threshold the point will be classified as an outlier, being removed from the point cloud. Thus, the performance of this filter greatly depends on the specified radius and minimum of neighbors threshold. This filter has the advantage of being easy to implement due to its simplicity but when applied on 3d LiDARS the fixed filter radius search becomes a problem because as the detection range increase the space between points will also increase due to the horizontal and vertical resolutions of lidar systems. Thus, the points detected by lidars at great distances most likely will be removed by this filter.

2.4.1.2 SOR

The SOR filter concept is somewhat similar to the ROR one, but instead of having a fixed search radius or a minimum of neighbors threshold as the ROR filter has, it instead computes the mean distance of each point to its neighboring point to considering the k-nearest neighbors. When these points are greater than the sum of the mean distance and the standard deviation they are classified as outliers. Similar to the ROR filter, the performance of the SOR filter depends on the number of nearest points, and the amount of times the stander deviation is calculated. ROR and SOR filters have the same disadvantages because both need to find the number of neighbors and that comes with a heavy computational cost, moreover because

of point cloud sparse distances, the greater the distance of the point to the LiDAR sensor, the higher the possibility of a point being removed as an outlier.

2.4.1.3 Voxel Grid Filter

Vox Grid Filter differs from the other filter in the way that it does not classify points as inliers or outliers, but it downsamples the number of points. All the points are inside a predefined 3D box in a 3D space and downsampled to an approximated voxel center point. Even though the Voxel Grid filter is a downsample filter, it can be considered a noise filter because in some cases, because some noise is random points with no neighbors and this filter will delete those. However, not only noise will be removed, because all points are downsampled, therefor this filter is only regarded as a downsampling filter, not a noise filter.

2.4.2 State fo the art filters:

New noise filters to 3d LiDAR point clouds are being developed, in this dissertation, two state-of-the-art filters will be studied and analyzed.

2.4.2.1 FCSOR FILTER

The Fast statistical outlier removal (FCSOR) [Balta et al., 2018] is an improved version of the SOR filter, This method is a somewhat junction of a voxel subsampling method and statistical outlier removal. By adding the voxel subsampling step the computational complexity reduces improving the run time requirements. This is done by reducing the number of clusters and perform some computations needed in parallel. However, the improvements shown in this filter are only performance-related, and still cannot achieve real-time capability.

2.4.2.2 DROR FILTER

The dynamic radius outlier removal (DROR) [Charron et al., 2018] filter was developed to compensate for the accuracy problems shown by the SOR and ROR filters in 3d LiDAR point clouds. The problem with 3d LiDAR point clouds is that the further the point measured the sparse the point cloud will be, being this far away point removed by both SOR and ROR filter. Instead of having a fixed radius like ROR filters, DROR has a dynamic one reducing distant point losses. This is done by changing the search radius for neighboring points as the distance measured increases. In the results present by the author, the DROR filter outperforms the conventional filters, in fact, it improves the accuracy by more than 90% compared to the conventional ROR. However, despite its good accuracy, it still has performance issues, having a high computational cost.

2.4.3 Filters Study.

In order to study the algorithms described in the previous section, a software tool was developed in c++, this tool was built on top of Point Cloud Library (PCL), which is an open-source library of algorithms for point cloud processing tasks and 3D geometry processing, such as occur in three-dimensional computer vision. The library contains algorithms for filtering, feature estimation, surface reconstruction, 3D registration, model fitting, object recognition, and segmentation. Each module is implemented as a smaller library that can be compiled separately (for example, libpcl_filters, libpcl_features, libpcl_surface, ...). PCL has its own data format for storing point clouds - PCD (Point Cloud Data) but also allows datasets to be loaded and saved in many other formats.

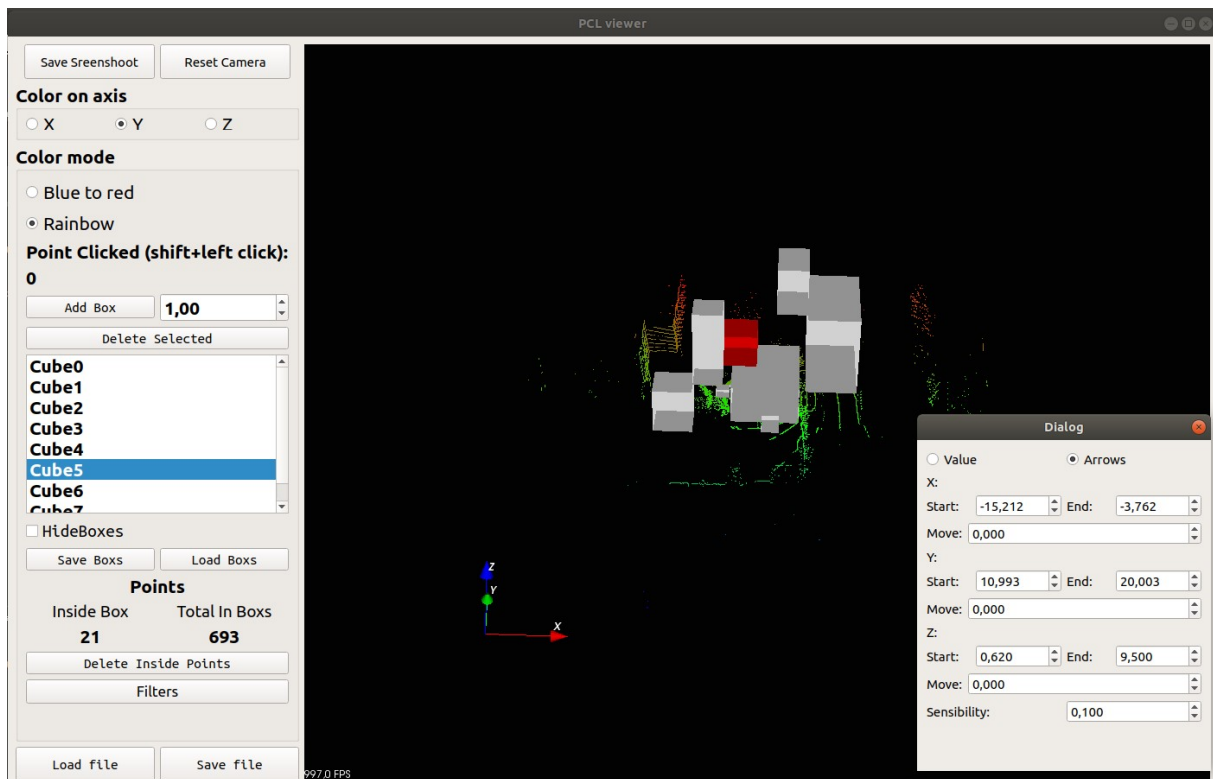


Figure 2.14: Software tool.

The software tool developed allows the user to analyze specific areas in a point cloud by adding boxes in the area to be analyzed. In the user-selected areas, the tool shows the total number of points inside the boxes allowing one to identify the number of points that can be considered noise. These boxes will also help to identify noise points to calculate some performance metrics by the algorithms.

First, the user needs to insert the point cloud that will be analyzed in the pcd or ply format, then the user needs to identify the noise areas with boxes. If the user wants to delete a certain area to not interfere in the measurements the user can delete the points inside a box.

2.4.3.1 Voxel

To configure the voxel filter, 3 parameters need to be set, this is the leaf size in x,y, and z. To achieve the best performance it was set to the size of 0.2 cm.

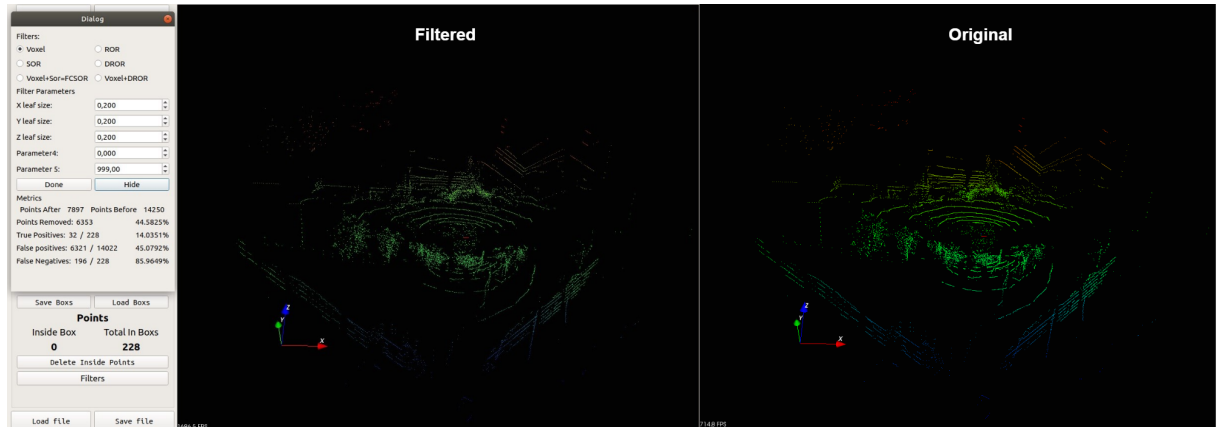


Figure 2.15: Voxel filter results.

As shown in 2.15 the voxel filter removes a lot of points from the point cloud, almost cutting the point cloud in half, but in terms of the noise points only removed 14% of the ones it needed to remove. This proves that this filter is not the most reliable for noise reduction from 3D point clouds, but in terms of the computational power, it reduces that for later filters by downsampling the point cloud.

2.4.3.2 ROR

The ROR filter has 2 parameters that need to be set, the radius for the neighbors search and the neighbor threshold, these values were set into consideration the LiDAR sensor that made the capture, a Velodyne 16p. Every point that in a 2 cm radius doesn't have 25 neighbors will be classified as outliers and removed.

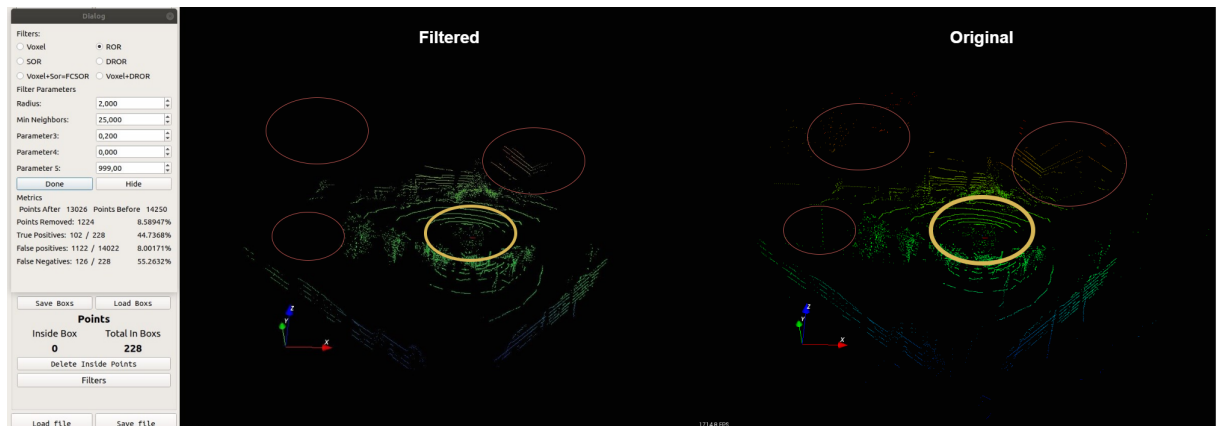


Figure 2.16: ROR filter results.

As shown in the image 2.16, we can see that the most scattered snow was removed, but the one that is denser wasn't removed. The ROR filter for this point cloud removed almost half of the signalized noise,

but, it also removed 8% of the point cloud, this percentage, as one can see represents the far aways points from the sensor, these points are still relevant to the object classifying algorithms.

2.4.3.3 SOR

Similar to the ROR filter, the SOR filter has 2 user-defined parameters. To set these parameters correctly, one needs to have the LiDAR system characteristics because it will determine the accuracy of this filter. In this case, the k means threshold described in the previous section was set to 1, and the threshold was set to 0.9 to achieve the best performance possible.

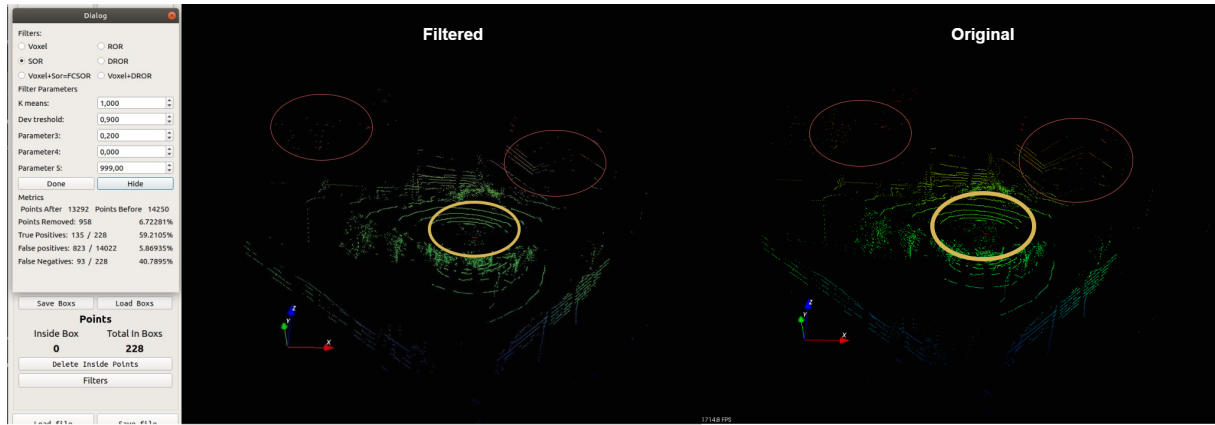


Figure 2.17: SOR filter results.

As shown in the image, the SOR filter performance is very similar to the ROR, but it has a little more accuracy, of the 228 points labeled as noise, in this case, noise generated by snow, the SOR filter removed 135 points, achieving a 59% success rate. However the same issue that happened with ROR filters happened with SOR filters too, the faraway points were removed, but, in this case, the number of points removed was more acceptable than the ROR filter.

2.4.3.4 FCSOR

The FSOR algorithm is a somewhat junction of the VOXEL filter and the SOR filter, it divides the point cloud into clusters and then applies the SOR filter to the clusters. To do that, the filter needs 3 parameters, the total number of clusters, which will calculate the leaf size of the box filter, the k means, and the threshold, that was talked about in the SOR filter.

The results of this filter were similar to the SOR filter, but that was already expected because the goal of this filter is to improve the computational performance of the SOR filter, it removed 24% of the point cloud by downsampling it, and the number of true positives was also somewhat equal to SOR filter, not improving the accuracy of the SOR filter. This filter also has the same disadvantage as ROR and SOR filters, which eliminates far away points that can be crucial for object recognition.

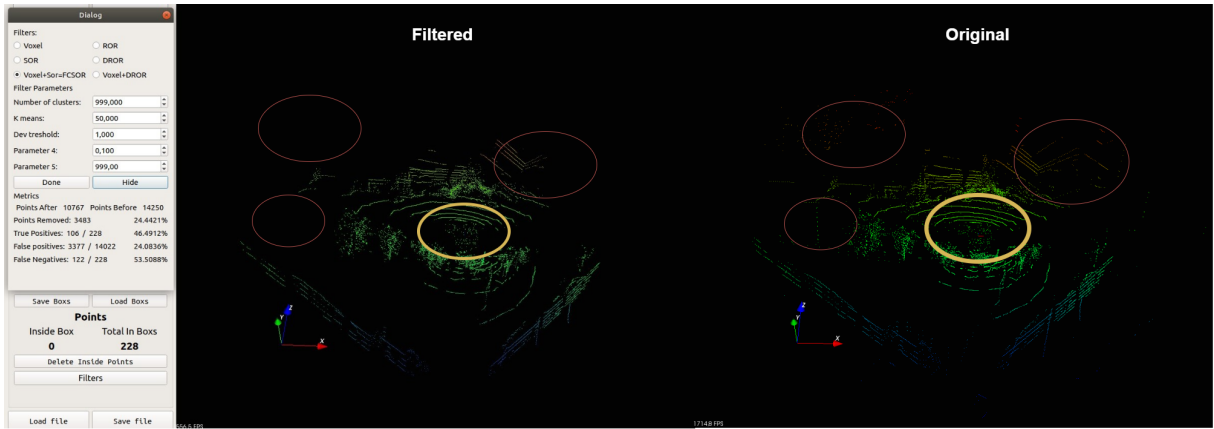


Figure 2.18: FCSOR filter results.

2.4.3.5 DROR

In the DROR filter the user needs to configure 4 parameters, the minimum search radius, similar to the ROR filter, this is the radius to check how many neighbors in that range, but in this case its a minimum to avoid using a very small search radius for points close to the vehicle. In figure 2.19 there is a parameter called Multi-Parameter, this parameter is a multiplication constant that is assigned to account for the increase in point spacing for surfaces that are not perpendicular to the lidar beams. The parameter minimum neighbors is the threshold where all the points without the minimum required will be classified as outliers. The last parameter is the angular resolution, which is a specification of the LiDAR sensor, in this case, because the sensor in use, a Velodyne 16vp has 0.1-0.4 horizontal resolution, 0.3 was chosen.

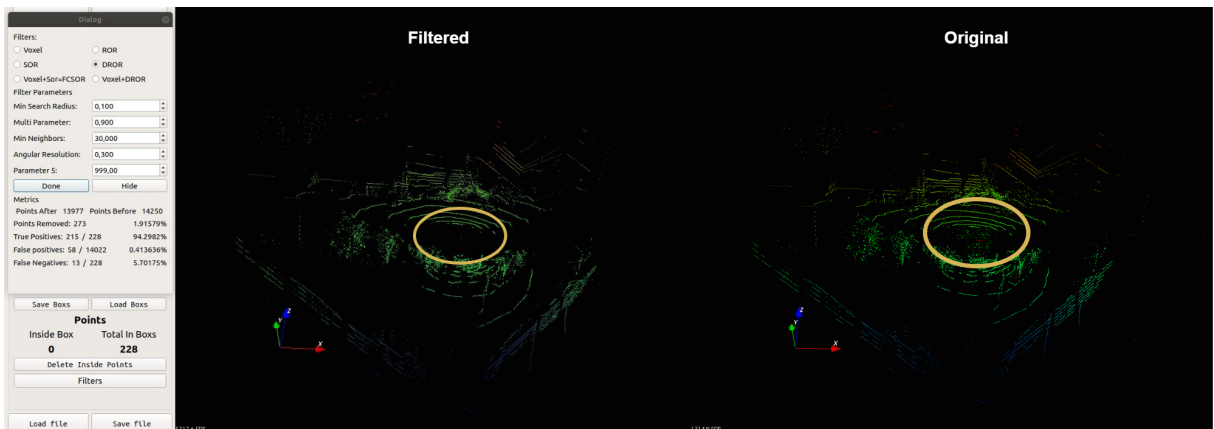


Figure 2.19: DROR filter results.

The results of this filter were very positive, in fact, it was better at close range than the original ROR filter which is the conceptual base of this filter. It achieved 95% accuracy, only missing 13 points that were too close to trees. As to false positives, it was the filter that better performed in this field, where it only removed 58 points that weren't labeled as snow, but some of them can be label as additional noise because they don't have any visible neighbors close to them.

2.4.4 Results

To compare the filter's performance a table with all the metrics, except for computing time, was made. The tests were all done with optimal parameters and all of them with the same frame.

	Voxel	ROR	SOR	DROR	FCSOR	FDROR
Points Removed	23%	9%	6%	2%	24%	20%
True Positives	10%	45%	59%	94%	70%	94%
False Positives	24%	8%	6%	1%	23%	19%
False Negatives	89%	55%	41%	5%	30%	5%

Table 2.1: Filters Results

By the table analysis, the best performing filter was the DROR, this filter outperformed all the other filters by a significant margin. It was also the filter that removed the least amount of points from the point cloud.

By the table analysis, the best performing filter was the DROR, this filter outperformed all the other filters

Platform and tools

3.1 ALFA

3.2 ROS

3.3 Zynq UltraScale+ MPSoC ZCU104

3.4 PCL

ALFA-Pd Architecture

4.1 ALFA-DVC

Chapter

5

ALFA-Pd Framework

Evaluation and Result

6.1 Filter performance

6.2 Hardware versus Software

Conclusion

7.1 Future work

Bibliography

- [Atanacio-Jiménez et al., 2011] Atanacio-Jiménez, G., González-Barbosa, J. J., Hurtado-Ramos, J. B., Ornelas-Rodríguez, F. J., Jiménez-Hernández, H., García-Ramírez, T., and González-Barbosa, R. (2011). LIDAR velodyne HDL-64E calibration using pattern planes. *International Journal of Advanced Robotic Systems*, 8(5):70–82.
- [Balta et al., 2018] Balta, H., Velagic, J., Bosschaerts, W., De Cubber, G., and Siciliano, B. (2018). Fast Statistical Outlier Removal Based Method for Large 3D Point Clouds of Outdoor Environments. *IFAC-PapersOnLine*, 51(22):348–353.
- [Biswas and Middleton, 1971] Biswas, A. K. and Middleton, W. E. K. (1971). Invention of the Meteorological Instruments. *Technology and Culture*, 12(2).
- [Burt et al., 2018] Burt, A., Disney, M., and Calders, K. (2018). Extracting individual trees from lidar point clouds using treeseg. *Methods in Ecology and Evolution*, 10(3):2041–210X.13121.
- [Byeon and Yoon, 2020] Byeon, M. and Yoon, S. W. (2020). Analysis of Automotive Lidar Sensor Model Considering Scattering Effects in Regional Rain Environments. *IEEE Access*, 8:102669–102679.
- [Charron et al., 2018] Charron, N., Phillips, S., and Waslander, S. L. (2018). De-noising of lidar point clouds corrupted by snowfall. In *Proceedings - 2018 15th Conference on Computer and Robot Vision, CRV 2018*, pages 254–261.
- [Eitel et al., 2016] Eitel, J. U., Höfle, B., Vierling, L. A., Abellán, A., Asner, G. P., Deems, J. S., Glennie, C. L., Joerg, P. C., LeWinter, A. L., Magney, T. S., Mandlburger, G., Morton, D. C., Müller, J., and Vierling, K. T. (2016). Beyond 3-D: The new spectrum of lidar applications for earth and ecological sciences. *Remote Sensing of Environment*, 186:372–392.
- [Gong et al., 2009] Gong, T., Wang, Y., Kong, L., Li, H., and Wang, A. (2009). Chaotic lidar for automotive collision warning system. *Zhongguo Jiguang/Chinese Journal of Lasers*, 36(9):2426–2430.
- [Goodin et al., 2019] Goodin, C., Carruth, D., Doude, M., and Hudson, C. (2019). Predicting the Influence of Rain on LIDAR in ADAS. *Electronics*, 8(1):89.
- [Granstrom et al., 2017] Granstrom, K., Renter, S., Fatemi, M., and Svensson, L. (2017). Pedestrian tracking using Velodyne data-Stochastic optimization for extended object tracking. In *IEEE Intelligent Vehicles Symposium, Proceedings*, pages 39–46.

- [Guo Liren et al., 2015] Guo Liren, Hu Yihua, Li Zheng, and Xu Shilong, (2015). Research on Influence of Acousto-Optic Frequency Shifter to Micro-Doppler Effect Detection. *Acta Optica Sinica*, 35(2):0212006.
- [Han et al., 2017] Han, X. F., Jin, J. S., Wang, M. J., Jiang, W., Gao, L., and Xiao, L. (2017). A review of algorithms for filtering the 3D point cloud. *Signal Processing: Image Communication*, 57.
- [Hasirlioglu et al., 2017] Hasirlioglu, S., Doric, I., Kamann, A., and Riener, A. (2017). Reproducible Fog Simulation for Testing Automotive Surround Sensors. In *2017 IEEE 85th Vehicular Technology Conference (VTC Spring)*, volume 2017-June, pages 1–7. IEEE.
- [Hasirlioglu et al., 2016] Hasirlioglu, S., Kamann, A., Doric, I., and Brandmeier, T. (2016). Test methodology for rain influence on automotive surround sensors. In *2016 IEEE 19th International Conference on Intelligent Transportation Systems (ITSC)*, pages 2242–2247. IEEE.
- [Heinzler et al., 2019] Heinzler, R., Schindler, P., Seekircher, J., Ritter, W., and Stork, W. (2019). Weather Influence and Classification with Automotive Lidar Sensors. *IEEE Intelligent Vehicles Symposium, Proceedings*, 2019-June:1527–1534.
- [Isermann et al., 2008] Isermann, R., Schorn, M., and Stählin, U. (2008). Anticollision system PRORETA with automatic braking and steering. *Vehicle System Dynamics*, 46(sup1):683–694.
- [Kutila et al., 2016] Kutila, M., Pyykonen, P., Ritter, W., Sawade, O., and Schaufele, B. (2016). Automotive LIDAR sensor development scenarios for harsh weather conditions. In *2016 IEEE 19th International Conference on Intelligent Transportation Systems (ITSC)*, pages 265–270. IEEE.
- [Li and Ibanez-Guzman, 2020] Li, Y. and Ibanez-Guzman, J. (2020). Lidar for Autonomous Driving: The Principles, Challenges, and Trends for Automotive Lidar and Perception Systems. *IEEE Signal Processing Magazine*, 37(4):50–61.
- [Lindner and Wanielik, 2009] Lindner, P. and Wanielik, G. (2009). 3D Lidar processing for vehicle safety and environment recognition. In *2009 IEEE Workshop on Computational Intelligence in Vehicles and Vehicular Systems, CIVVS 2009 - Proceedings*.
- [Lundquist et al., 2013] Lundquist, C., Granstrom, K., and Orguner, U. (2013). An Extended Target CPHD Filter and a Gamma Gaussian Inverse Wishart Implementation. *IEEE Journal of Selected Topics in Signal Processing*, 7(3):472–483.
- [Moosmüller et al., 2003] Moosmüller, H., Mazzoleni, C., Barber, P. W., Kuhns, H. D., Keislar, R. E., and Watson, J. G. (2003). On-Road Measurement of Automotive Particle Emissions by Ultraviolet Lidar and Transmissometer: Instrument. *Environmental Science and Technology*, 37(21):4971–4978.

- [Ogawa et al., 2011] Ogawa, T., Sakai, H., Suzuki, Y., Takagi, K., and Morikawa, K. (2011). Pedestrian detection and tracking using in-vehicle lidar for automotive application. In *2011 IEEE Intelligent Vehicles Symposium (IV)*, pages 734–739. IEEE.
- [Panurak et al., 2009] Panurak, W., Thanok, S., and Parnichkun, M. (2009). Adaptive cruise control for an intelligent vehicle. In *2008 IEEE International Conference on Robotics and Biomimetics, ROBIO 2008*, pages 1794–1799.
- [Patole et al., 2017] Patole, S. M., Torlak, M., Wang, D., and Ali, M. (2017). Automotive radars: A review of signal processing techniques. *IEEE Signal Processing Magazine*, 34(2):22–35.
- [Raj et al., 2020] Raj, T., Hashim, F. H., Huddin, A. B., Ibrahim, M. F., and Hussain, A. (2020). A survey on LiDAR scanning mechanisms.
- [Rakotovao et al., 2016] Rakotovao, T., Mottin, J., Puschini, D., and Laugier, C. (2016). Multi-sensor fusion of occupancy grids based on integer arithmetic. In *2016 IEEE International Conference on Robotics and Automation (ICRA)*, volume 2016-June, pages 1854–1859. IEEE.
- [Raschofer and Gresser, 2005] Raschofer, R. H. and Gresser, K. (2005). Automotive Radar and Lidar Systems for Next Generation Driver Assistance Functions. *Advances in Radio Science*, 3:205–209.
- [Raschofer et al., 2011] Raschofer, R. H., Spies, M., and Spies, H. (2011). Influences of weather phenomena on automotive laser radar systems. *Advances in Radio Science*, 9:49–60.
- [Redington, 1962] Redington, R. (1962). Elements of infrared technology: Generation, transmission and detection. *Solid-State Electronics*, 5(5):361.
- [Ring, 1963] Ring, J. (1963). The Laser in Astronomy. *New Scientist*, 344.
- [Rusu and Cousins, 2011] Rusu, R. B. and Cousins, S. (2011). 3D is here: Point Cloud Library (PCL). *Proceedings - IEEE International Conference on Robotics and Automation*, (May 2011).
- [Shin et al., 2017] Shin, H., Kim, D., Kwon, Y., and Kim, Y. (2017). Illusion and dazzle: Adversarial optical channel exploits against lidars for automotive applications. In *Lecture Notes in Computer Science (including subseries Lecture Notes in Artificial Intelligence and Lecture Notes in Bioinformatics)*, volume 10529 LNCS, pages 445–467.
- [Süss et al., 2016] Süss, A., Rochus, V., Rosmeulen, M., and Rottenberg, X. (2016). Benchmarking time-of-flight based depth measurement techniques. In *Smart Photonic and Optoelectronic Integrated Circuits XVIII*, volume 9751, page 975118.
- [Synge, 1930] Synge, E. (1930). XCI. A method of investigating the higher atmosphere. *The London, Edinburgh, and Dublin Philosophical Magazine and Journal of Science*, 9(60):1014–1020.

- [Tuve et al., 1935] Tuve, M. A., Johnson, E. A., and Wulf, O. R. (1935). A new experimental method for study of the upper atmosphere. *Journal of Geophysical Research*, 40(4):452.
- [Vargas Rivero et al., 2020] Vargas Rivero, J. R., Gerbich, T., Teiluf, V., Buschardt, B., and Chen, J. (2020). Weather Classification Using an Automotive LIDAR Sensor Based on Detections on Asphalt and Atmosphere. *Sensors*, 20(15):4306.
- [Zhou and Sun, 2019] Zhou, Z. Q. and Sun, L. (2019). Metamorphic testing of driverless cars. *Communications of the ACM*, 62(3):61–67.